PRACTICAL SUPERCONDUCTOR DEVELOPMENT

FOR ELECTRICAL POWER APPLICATIONS

ARGONNE NATIONAL LABORATORY

QUARTERLY REPORT FOR THE PERIOD ENDING SEPTEMBER 30, 2002

This is a multiyear experimental research program that focuses on improving relevant material properties of high-T_c superconductors (HTSs) and developing fabrication methods that can be transferred to industry for production of commercial conductors. The development of teaming relationships through agreements with industrial partners is a key element of the Argonne (ANL) program.

Technical Highlights

MgO films prepared by inclined substrate deposition (ISD) on Hastelloy C (HC) substrates were shown to exhibit fully developed biaxial texture within ≈1.5 min at a deposition rate of 50 Å/sec, and the biaxial texture was shown to be independent of the surface roughness of the HC substrates. The orientation relationship between $YBa_2Cu_3O_{7-\delta}$ (YBCO) and yttria-stabilized zirconia (YSZ)- and ceria (CeO_2)-buffered ISD MgO was analyzed. A YBCO-coated conductor with the ISD MgO architecture exhibited a sharp superconducting transition (T_c = 91 K) and a transport J_c of 5.5 x 10^5 A/cm^2 at 77 K in self-field. In addition, an empirical correlation was developed that allows calculation of electric field strength for a range of temperature and current density that is relevant to the operation of practical superconductor devices.

Fabrication of Coated Conductors by ISD MgO Process

Previous reports [1-3] described MgO films that were deposited on Hastelloy C (HC) substrates by the ISD method. ISD MgO films consist of columnar grains that stand nearly perpendicular to the substrate surface and are terminated by MgO (002) planes. Because the [002] planes are tilted with respect to the substrate normal, ISD MgO films exhibit a roof-tile structure with a surface roughness of ≈28 nm. This roughness is reduced to ≈9 nm by depositing an additional thin layer of MgO at a substrate inclination α of 0°. Deposition of this homoepitaxial MgO layer also improves the biaxial texture of the films, giving full width at half maximums (FWHMs) of 9.2 and 5.4° for the MgO (002) ϕ- and ω-scans, respectively. Before YBCO is deposited on the MgO films, buffer layers of YSZ and CeO_2 are deposited by pulsed laser deposition (PLD). In this report, we elucidate the orientation relationship between YBCO and the MgO template. We also show that the biaxial alignment in MgO films develops rapidly and is not affected by the surface roughness of the HC substrates (up to a surface roughness of ≈15 nm). In addition, we briefly describe the surface morphology of the YSZ and CeO_2 buffer layers.

Mechanically polished HC coupons (≈0.1 mm x ≈5 mm x 1 cm) were used as the substrates for deposition of ISD MgO template films, YSZ and CeO_2 buffer layers, and YBCO films. A root-mean-square (RMS) surface roughness of 2-3 nm was measured by atomic force microscopy (AFM) on HC substrates that were polished with 0.25-μm diamond paste. To evaluate the effect of surface roughness, we also polished HC substrates with various coarser grinding media to obtain surface roughnesses up to 15 nm. MgO thin films were grown from an MgO source by electron beam (e-beam) evaporation with an experimental apparatus that is described elsewhere [2]. Fused lumps of MgO (Alfa Aesar, 99.95% metals basis, 3-12-mm pieces) were used as the target material. Substrates were mounted on a sample stage that can be tilted above the e-beam evaporator to give a range of substrate inclinations α, the angle between the substrate normal and the evaporation direction. In this study, α was ≈55°. High-purity oxygen was flowed into the system at ≈3 sccm during film deposition. The base pressure of the system was 1×10^{-7} torr and rose to ≈2×10^{-5} torr during deposition. A quartz crystal monitor beside the sample stage monitored and controlled the deposition rate. Deposition rates of 20-100 Å/sec were used, and the substrate temperature during deposition was maintained between room temperature and 50°C. After depositing the ISD films, a dense, thin, layer of MgO was deposited at elevated temperature (≈700°C) and with α ≈ 0°. Because this layer exibits the same crystalline texture as the ISD MgO film underneath, it is referred to as the homoepitaxial MgO layer.

Buffer layers and YBCO films were deposited by PLD with a Lambda Physik LPX 210i excimer laser, in which a Kr-F_2 gas premixture was the lasing medium. Figure 1 shows a schematic illustration of the PLD system, which uses an optical beam raster to produce films with good uniformity over a broad area. The laser beam of the system is focused at the target through a quartz lens (1000-mm focal length) that has an anti-reflective coating. The beam is reflected by a mirror that is mounted as part of the beam raster and hits the target at an incident angle 45°. The rotating target carrousel carries four targets to accommodate the ablation of multiple layers without breaking vacuum. Commercial targets (99.999% pure, 45 mm in diameter x 6 mm thick) from Superconductive Components were used. Substrates were attached to a heated sample stage with silver paste and heated to a high temperature (700-800°C) during deposition. The base pressure of the PLD chamber was ≈1×10^{-5} Torr. An operating pressure of 100-300 mTorr was maintained by flowing ultra-high-purity oxygen at ≈10 sccm and pumping the chamber with a molecular turbo pump. The spot size of the laser beam on the rotating target was ≈12 mm^2, which gave an energy density of ≈2.0 J/cm^2. The distance between the target and the substrates was ≈7 cm.

The superconducting critical transition temperature (T_c) and critical current density (J_c) were determined by the inductive method, in which superconductor samples are placed between a primary and a secondary coil, each with an inner

diameter of ≈1 mm

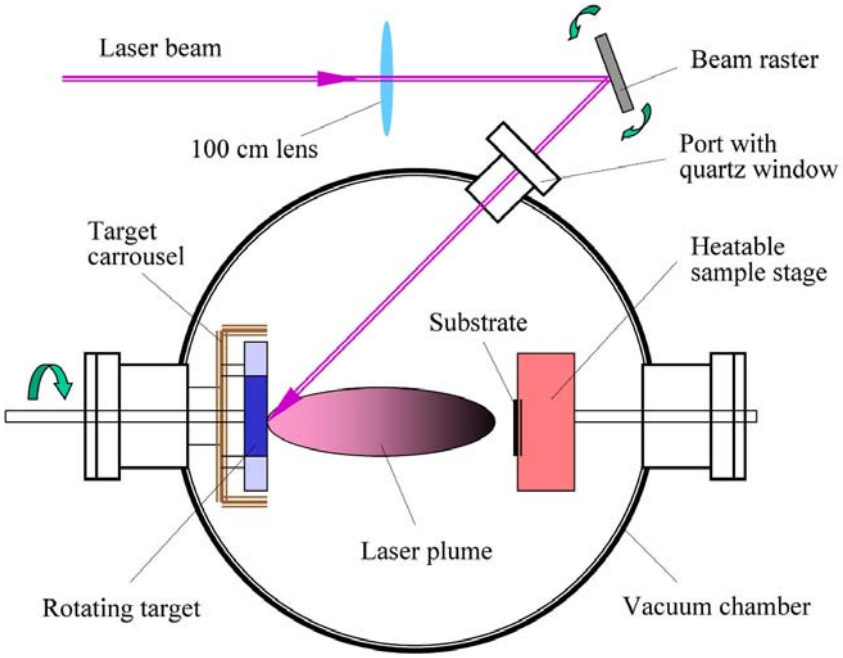

Fig. 1. Schematic illustration of PLD system.

and an outer diameter of ≈5 mm. An alternating current of 1 kHz is introduced into the primary coil and detected by the secondary coil with a lock-in amplifier (Stanford Research Systems SR830 DSP). The transport J_c of selected samples was measured by the four-point method at 77 K in liquid nitrogen using an 1-μV/cm criterion. Samples used for transport measurements were first coated with 2-μm-thick silver by e-beam evaporation and then annealed in flowing high-purity oxygen at 400°C for 2 h.

Film textures were characterized by X-ray diffraction pole figure analysis with Cu-K_α radiation. The in-plane textures of ISD MgO films and subsequently deposited buffer layers were characterized by the FWHMs of ϕ-scans for the (002) reflections, and the out-of-plane textures were characterized by the FWHM of ω-scans at the [001] pole for the same reflection. The in-plane texture of YBCO was measured by the FWHM of the YBCO (103) ϕ-scan, and the out-of-plane texture was measured by the FWHM of the YBCO (005) ω-scan. The surface morphology of individual layers was examined with an Hitachi S-4700-II scanning electron microscope (SEM), and selected-area diffraction (SAD) with a Philips CM30 transmission electron microscope (TEM) was used to derive the relationship of the crystalline orientations among the ISD MgO template, YSZ and CeO_2 buffer, and YBCO films. Surface roughness was measured in the tapping mode with a Digital Instruments Dimension 3100 SPM AFM.

The development of biaxial texture in MgO films was studied as a function of film thickness. ISD MgO films of various thickness were grown, then a homoepitaxial MgO layer (thickness ≈ 0.5 μm) was deposited on each of the films, and the FWHM of a MgO (002) ϕ-scan was measured for each film. The homoepitaxial layer was added to sharpen the biaxial texture of the film and reduce its surface roughness. The effect of the homoepitaxial layer on surface roughness is shown in the AFM images of Fig. 2. Figure 3 shows that the in-plane texture quickly improves as the ISD MgO layer is made thicker. As the ISD MgO film thickness increases from 0.1 to 0.5 μm, the ϕ-scan FWHM decreases from ≈21.5° to ≈10.5°; the FWHM stabilizes at ≈9° for a thickness >0.5 μm. At a deposition rate of 50 Å/sec, the texture is fully developed within ≈1.5 min.

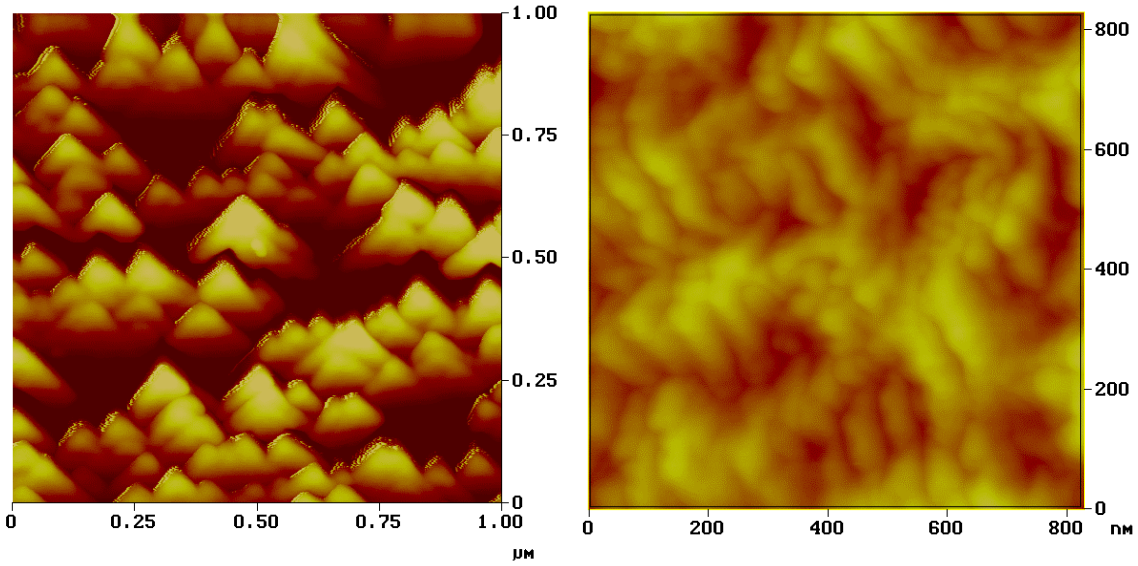

(a) (b)

Fig. 2. AFM images of (a) ISD MgO and (b) homoepitaxial MgO films.

The effect of surface roughness on biaxial texture in ISD MgO films was evaluated. HC substrates were polished with various coarse (compared to 0.25 μm diamond paste that is typically used) grinding media to obtain surface roughnesses that ranged up to 15 nm. Figure 4 shows that the biaxial texture of ISD MgO films is independent of substrate surface roughness up to a RMS surface roughness of 15 nm for ≈2-μm-thick ISD MgO films.

YSZ and CeO_2 films were epitaxially grown on top of the homoepitaxial MgO film by PLD under the conditions listed in Table 1. The thickness of the YSZ and CeO_2 layers was ≈200 nm and ≈10 nm, respectively. The CeO_2 and YSZ layers both have a cube-on-cube epitaxial relationship with the ISD MgO template film. Figure 5 shows (002) pole figures for the MgO, YSZ, and CeO_2 layers. The pole figures show that the c-axes for the YSZ and CeO_2 buffer films are both tilted at the same angle (≈32°) as the

ISD MgO template film, and they suggest a cube-on-cube epitaxial relationship in which CeO_2<100> // YSZ<100> // MgO<100> and CeO_2<010> // YSZ<010> // MgO<010> or

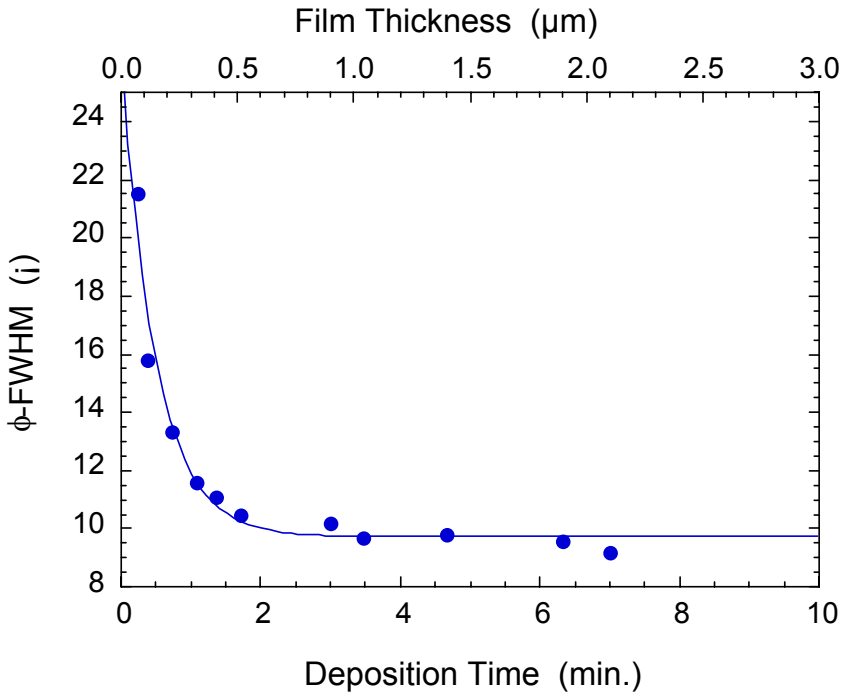

Fig. 3. Texture development in ISD MgO film.

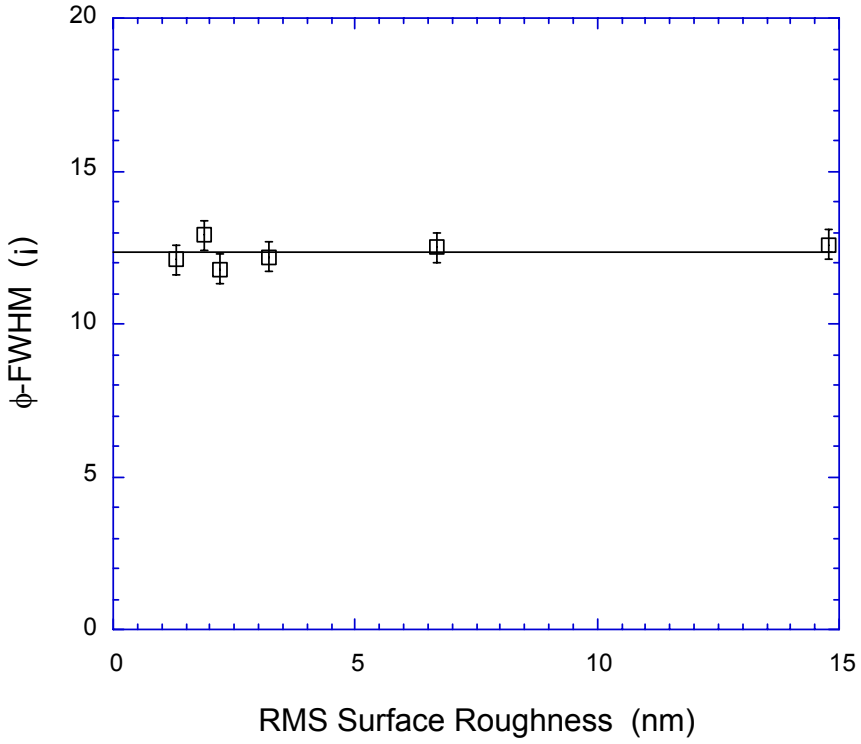

Fig. 4. In-plane texture as a function of substrate surface roughness for 2-μm-thick ISD MgO films.

Table 1. Conditions used for epitaxial growth of YSZ and CeO_2 buffer layers by PLD

Laser wavelength	248 nm (Kr-F)
Repetition rate	2-8 Hz
Pulse width	25 ns
Energy density	1-3 J/cm^2
Substrate temperature	700-800°C
Operating pressure	1-100 mtorr
Oxygen flow rate	1-10 sccm
Target-to-substrate distance	4-8 cm

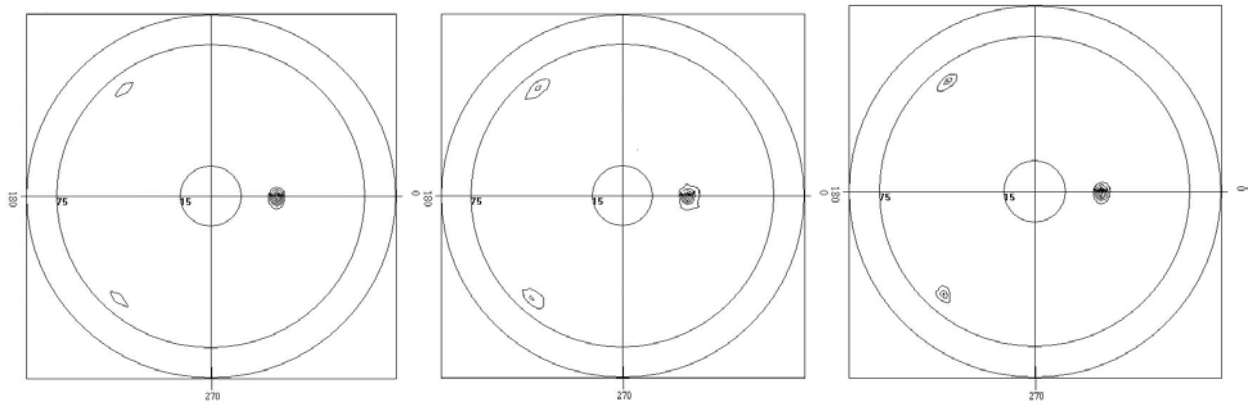

(a) (b) (c)

Fig. 5. X-ray pole figures for (a) MgO (002), (b) YSZ (002), and (c) CeO_2 (002), showing cube-on-cube epitaxial relationship among CeO_2, YSZ buffer layers, and ISD MgO film underneath.

CeO_2<001> // YSZ<001> // MgO<001>. This epitaxial relationship was confirmed by TEM studies [4]. The FWHMs of (002) ϕ-scans for MgO, YSZ, and CeO_2 were 9.2, 8.8, and 8.0°, respectively.

Figure 6 shows plan-view SEM images of YSZ and CeO_2 buffer layers that were grown on an ISD MgO template film. The "roof-tile" morphology that is evident on the surface of the YSZ layer (Fig. 6a) is similar to that observed on ISD MgO films; however, the "roof tile" appearance is hardly visible (Fig. 6b) after deposition of the CeO_2 layer. Examination with the AFM shows that deposition of the buffer layers has decreased the surface roughness to an RMS of ≈8 nm for both the YSZ and CeO_2 films. Despite the improvement in surface smoothness, the CeO_2 films contained several defects such as pits and particles protruding from the surface. These defects are being studied further to determine their influence on the superconducting properties of a YBCO film that is deposited on top of it.

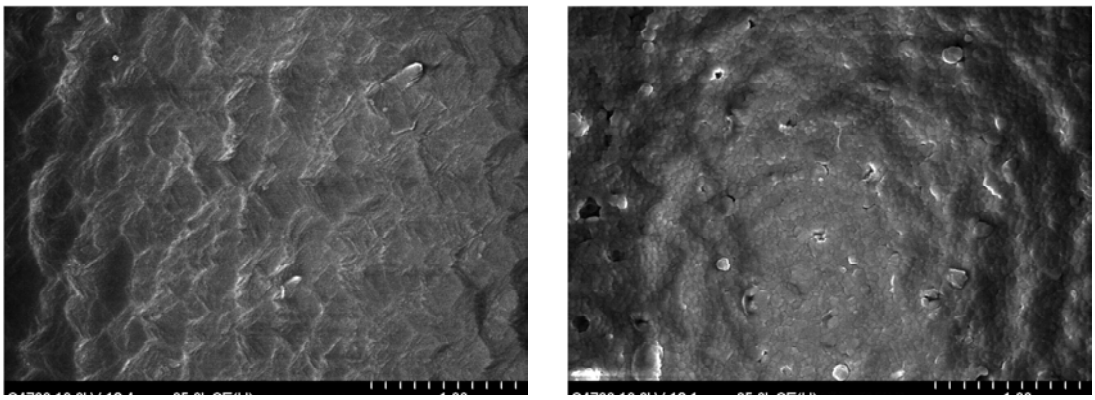

Fig. 6. Plan-view SEM images of (a) YSZ and (b) CeO_2 buffer layers deposited on ISD MgO template film.

Figure 7 shows X-ray diffraction patterns of a YBCO film that was deposited on a YSZ- and CeO_2-buffered ISD MgO substrate. The patterns were collected in two sample orientations that are indicated by insets in the patterns. In the normal orientation (Fig. 7a), only YBCO (00*l*) peaks are seen, which indicates that the c-axis of YBCO is parallel to the substrate normal. No diffraction peaks are observed for MgO, YSZ, or CeO_2 in this orientation, because these layers are tilted with respect to the substrate normal and the Bragg diffraction condition is not satisfied. In the tilted orientation (Fig. 7b), the sample is rotated to observe the MgO (002) reflection. In this orientation, the (002) reflections for YSZ and CeO_2 are also observed, indicating that they have the same orientation as MgO, whereas the (00*l*) peaks of YBCO are absent.

The orientation relationship between YBCO and YSZ- and CeO_2-buffered ISD MgO was analyzed. Because the lattice match between the YBCO pseudo-cell and and CeO_2 is very close, and the YBCO unit cell is larger than that of CeO_2, the X-ray diffraction peaks for YBCO overlap those of CeO_2. Therefore, the crystalline texture of CeO_2 is difficult to analyze after YBCO has been deposited. However, because the YSZ and CeO_2 buffer layers grow epitaxially on MgO, their orientation relationship with YBCO should be equivalent to that between YBCO and the MgO template layer, assuming that the orientations of YSZ and CeO_2 do not change during the deposition of YBCO.

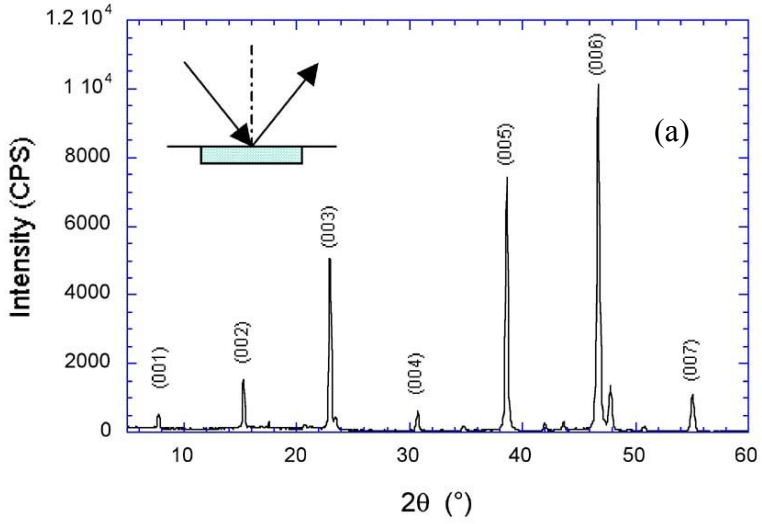

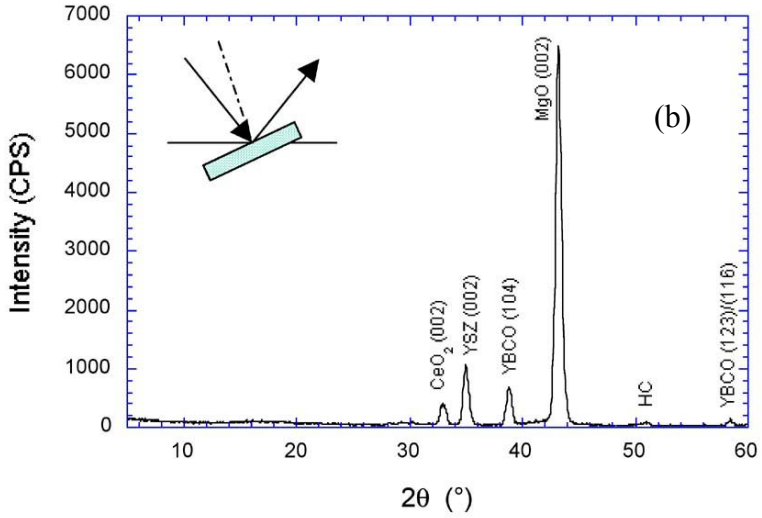

Fig. 7. X-ray diffraction patterns of YBCO film deposited on YSZ- and CeO_2-buffered ISD MgO substrate at (a) normal arrangement and (b) MgO (002) pole.

The YBCO (005) pole figure (Fig. 8a) shows a single pole at its center, whereas the YBCO (103) pole figure shows four evenly distributed poles (Fig. 8b). This confirms that the YBCO films deposited on YSZ- and CeO_2-buffered ISD MgO substrates are biaxially textured, with the c-axis oriented normal to the substrate. The MgO (002) and (220) pole figures, (Figs. 8c and 8d, respectively) show that the MgO template is also biaxially textured, but its c-axis is tilted with respect to the substrate normal. From the relative positions of their poles, we derived the following unique orientation relationship: YBCO<100> // MgO<111> and YBCO<010> // MgO<110>.

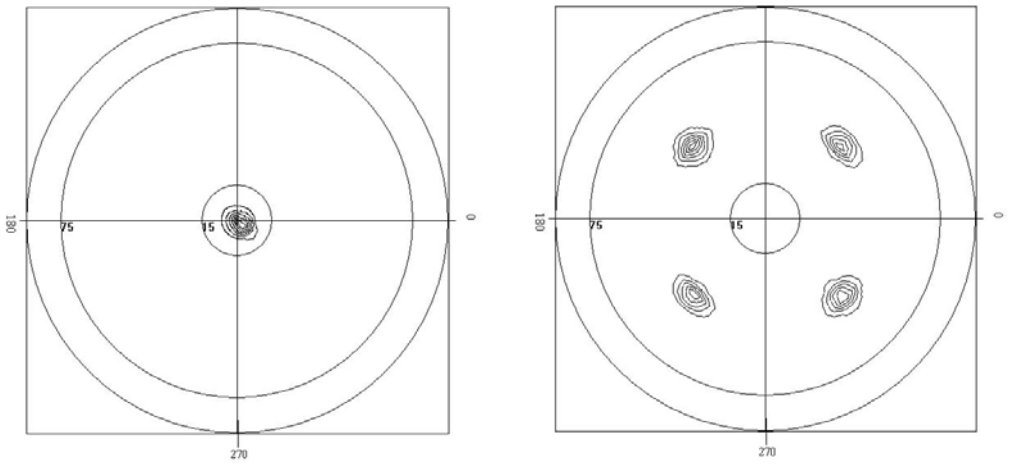

(a) (b)

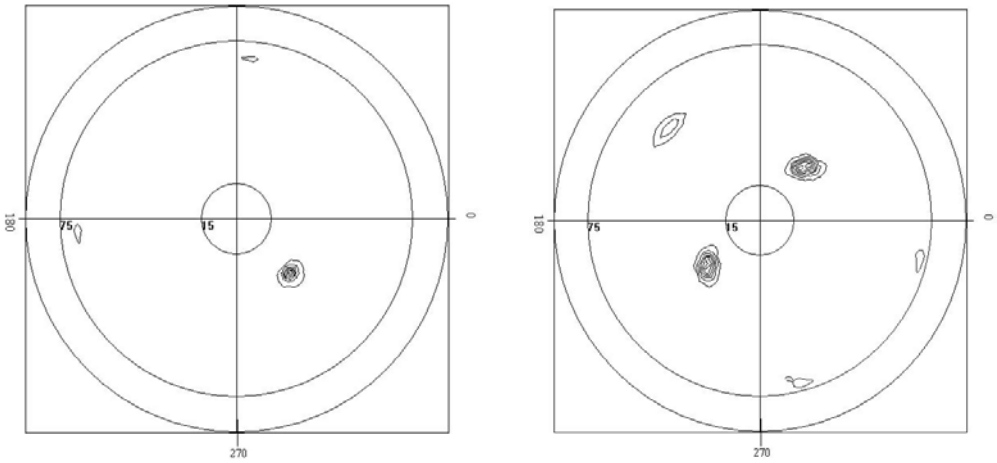

(c) (d)

Fig. 8. X-ray pole figures for (a) YBCO (005), (b) YBCO (103), (c) MgO (002), and (d) MgO (220) measured on the same sample.

The orientation relationship between YBCO and YSZ- and CeO_2-buffered ISD MgO was confirmed by TEM. Figure 9 shows a cross-sectional image of YBCO on YSZ- and CeO_2-buffered ISD MgO on HC; Fig. 10 shows results from SAD along the [111] zone axis for MgO and YSZ. These results confirm the relationship that was derived from the pole figures, but this relationship differs from the one that was reported earlier [2] where YBCO<001> // MgO<001> and YBCO<100> // MgO<100>. We believe that the difference in the orientation relationship is the result of differences in the YBCO growth conditions and the buffer layer architecture.

YBCO-coated conductors that were fabricated with the ISD MgO architecture (with the c-axis of YBCO normal to the substrate) exhibited a sharp superconducting

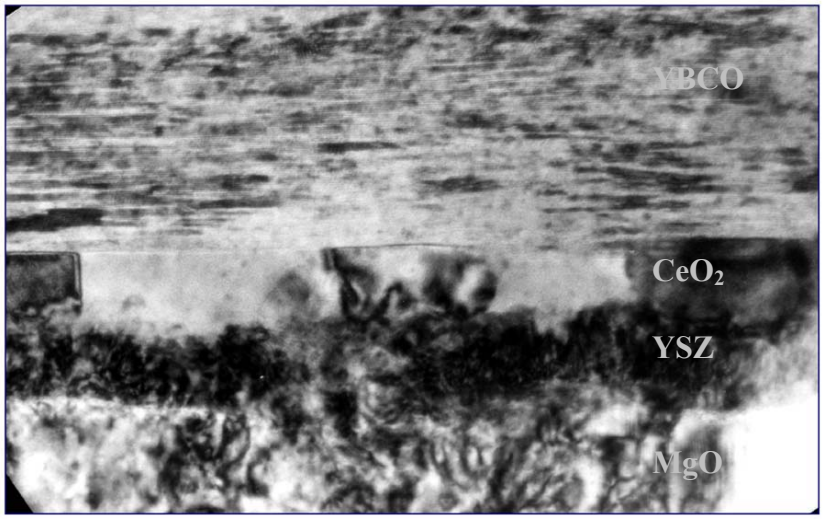

Fig. 9. TEM cross-sectional image of YBCO film deposited on YSZ- and CeO_2-buffered ISD MgO on HC substrate.

transition with T_c = 91 K. As shown in Fig. 11, a transport J_c of 5.5 x 10^5 A/cm^2 was measured at 77 K in self-field on a sample that was 0.46 μm thick, 4 mm wide, and 1 cm long.

An Empirical Correlation for E(J, T) of Melt-Cast BSCCO-2212

A basic property of superconductors is electric field strength (E), which is a function of current density (J), temperature (T), and magnetic flux density (B). The magnetic flux density is the sum of the applied field and the self-field due to the current density. If there is no applied field, the electric field strength can be considered a function of the current density and temperature, E = E(J,T). In practical applications of high-T_c superconducting devices, information on E(J,T) is often needed over a range of current density and temperature. For example, in a resistive fault current limiter, the superconductor heats up substantially during a fault. Even for the so-called superconductor-shielded-core reactor (SSCR), which is often known as an inductive fault current limiter, the superconductor tube heats up considerably during a fault. To determine accurately the voltage drop across the fault current limiter during a fault, the complete map of E as a function of J and T must be known. Recently, Cha and Askew [5-7] reported that thermal and magnetic diffusion is the mechanism for field penetration of a superconductor tube when it is subjected to a pulsed magnetic field. Similarly, thermal and magnetic diffusion will be important for the SSCR because it is based on the shielding capability of a superconductor tube. Furthermore, thermal and magnetic diffusion are also important for trapping of the magnetic field in a superconductor pellet with a pulsed current supply [8-10]. To model the coupled thermal and magnetic diffusion and understand how the magnetic field and the temperature of the superconductor evolve during a transient, complete information on E(J,T) must be known, presumably from experimental data. However, these kinds of data are hard to find because most of the researchers only measure the E/J characteristics at one or two temperatures (mostly at 77 K).

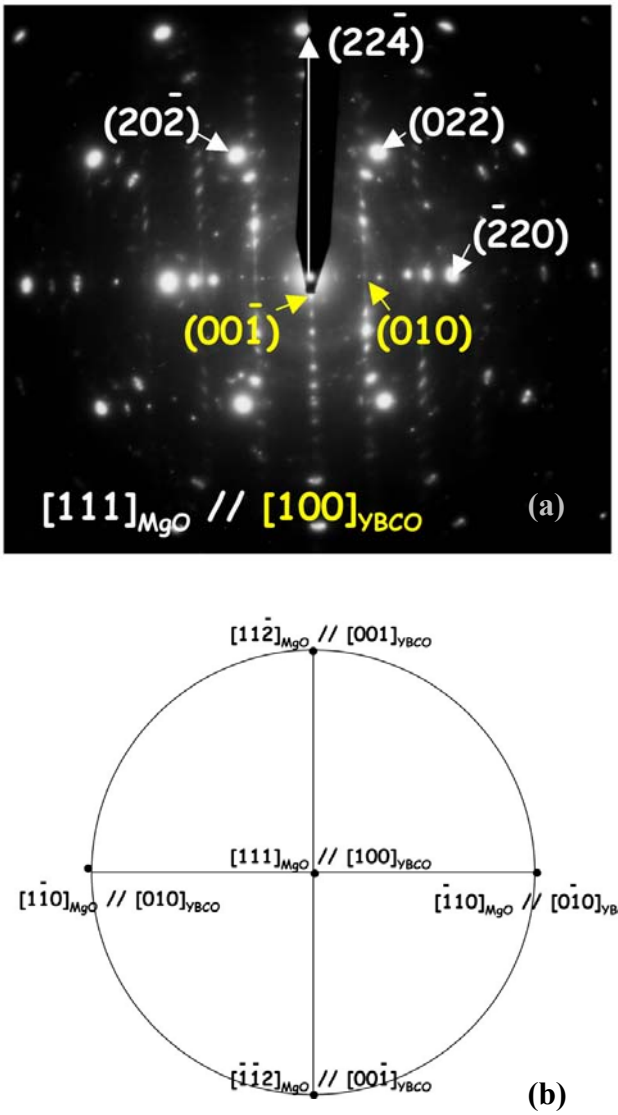

Fig. 10. (a) TEM selected area diffraction along MgO [111] zone axis, and (b) a stereograph projection showing orientation relationship between YBCO and MgO films.

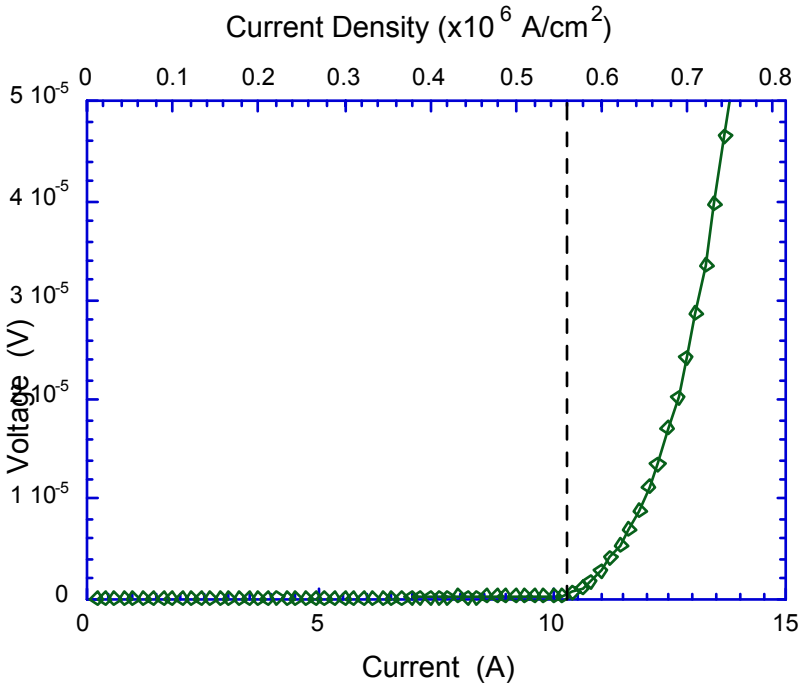

Fig. 11. Transport J_c of YBCO on ISD MgO measured at 77 K in self-field.

In this report, we use the E/J data for a melt-cast BSCCO-2212 superconductor at two temperatures (77 and 87 K) to develop an empirical correlation for E(J,T) that can then be used to calculate E from 77 K to the critical temperature of 90-92 K. With this correlation, the electric field strength can then be calculated for a range of temperature and current density that is relevant to the operation of practical devices made from melt-cast BSCCO-2212 superconductors. The correlation is based in part on the theory of magnetic relaxation [11], and the general form of the correlation may be applicable to other high-T_c superconductors.

The experimental data were reported previously [12]. The superconductor is a melt-cast BSCCO rod made by Hoechst (now called Nexans). The diameter of the rod is 7.85 mm. The standard four-point measurement technique was employed for all of the tests with a distance of 87 mm between the voltage taps. The critical current was defined by the 1 μV/cm criterion. Braided current leads were soldered to the ends of the sample and connected to a pulsed power supply. A pulsed current with a duration of 400 ms (square wave) was used in the experiment. The tests at 77 K were conducted in an open dewar with liquid nitrogen; tests at 87 K were conducted in the same open dewar with liquid argon.

Figure 12 shows the V/I characteristics of a melt-cast processed BSCCO-2212 rod at 77 and 87 K. The critical current defined at 77 K is one order of magnitude larger than that at 87 K. The tests were conducted by gradually increasing the current density

and were terminated when the heating effect became appreciable. The range of experimental data for current density is relatively small at 87 K when compared to that at 77 K, because the J_c is much smaller at 87 K, while dissipation and heating in the superconductor are much larger. Therefore, it was necessary to terminate the experiment at 87 K at a relatively small current density.

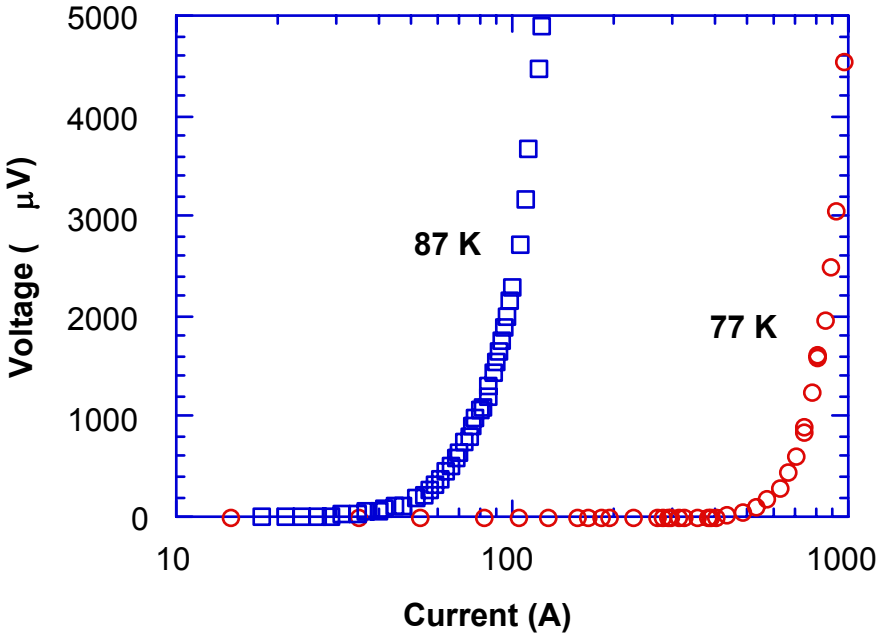

Fig. 12. Measured E/J characteristics at 77 and 87 K for a melt-cast processed BSCCO-2212 superconductor.

High-T_c superconductors usually obey the so-called power law,

$$E/E_c = (J/J_c)^n, \tag{1}$$

where both E_c and J_c can be functions of temperature, and the exponent n is a strong function of temperature and can vary widely for various high-T_c superconductors. The power law is the result of magnetic relaxation and can be explained in terms of the Anderson-Kim model for thermally activated flux creep [11],

$$E(J) = E_c \exp[-U(J)/kT]. \tag{2}$$

If a logarithmic dependence of U on J is assumed,

$$U(J) = U_0 \ln(J_c/J) \tag{3}$$

and the result is the power law shown in Eq. 1, with

$$n = U_0/kT. \quad (4)$$

The parameter U_0 is independent of J but can be a function of T.

The theory of flux creep or magnetic relaxation is of little help in determining the temperature dependence of U_0. However, we know that the superconductor becomes an Ohmic conductor when T approaches T_c, so the exponent n should approach one and the E/J relationship should become linear. The following equation satisfies this condition:

$$n = U_0/kT = 1 + C_0 \ln(T_c/T), \quad (5)$$

where C_0 is a constant. It is easily shown that n = 1 when T = T_c. From the experimental data at 77 and 87 K, it was found that $C_0 \cong 40$. Equation 1 can be written as

$$E(J,T) = f(T) \times J^n = f(T) \times J^{[1 + 40 \ln(T_c/T)]}, \quad (6)$$

where the function f depends only on temperature and is equal to

$$f(T) = E_c/(J_c)^n . \quad (7)$$

After some manipulation and with application of the data in Fig. 12 to determine the constant coefficients (detailed development can be found in reference [13]), the final correlation for E(J,T) becomes

$$E(J,T) = (39.236680 - 0.856427T + 0.004673T^2) \times 10^{2(T-89)} \times J^{[1 + 40 \ln(T_c/T)]}, \quad (8)$$

where T is the temperature in Kelvin, the current density J is in A/cm^2, and the electrical field strength E is in μV/cm. Figure 13 shows the value of E(J,T) calculated from Eq. 8 and the experimental data at 77 and 87 K. The calculated values appear to match the experimental data at 77 and 87 K fairly well; and thus, the calculation is capable of predicting the general trend of E as a function of current density at other temperatures between 77 and 92 K. The correlation developed here is specifically for the melt-cast BSCCO-2212 superconductor, because the coefficients were determined from the data in Fig. 12. The general form of E(J,T), given by Eqs. 2-7, may, however, be applicable to other bulk high-T_c superconductors, because it is based, in part, on the general theory of magnetic relaxation (thermally activated flux creep).

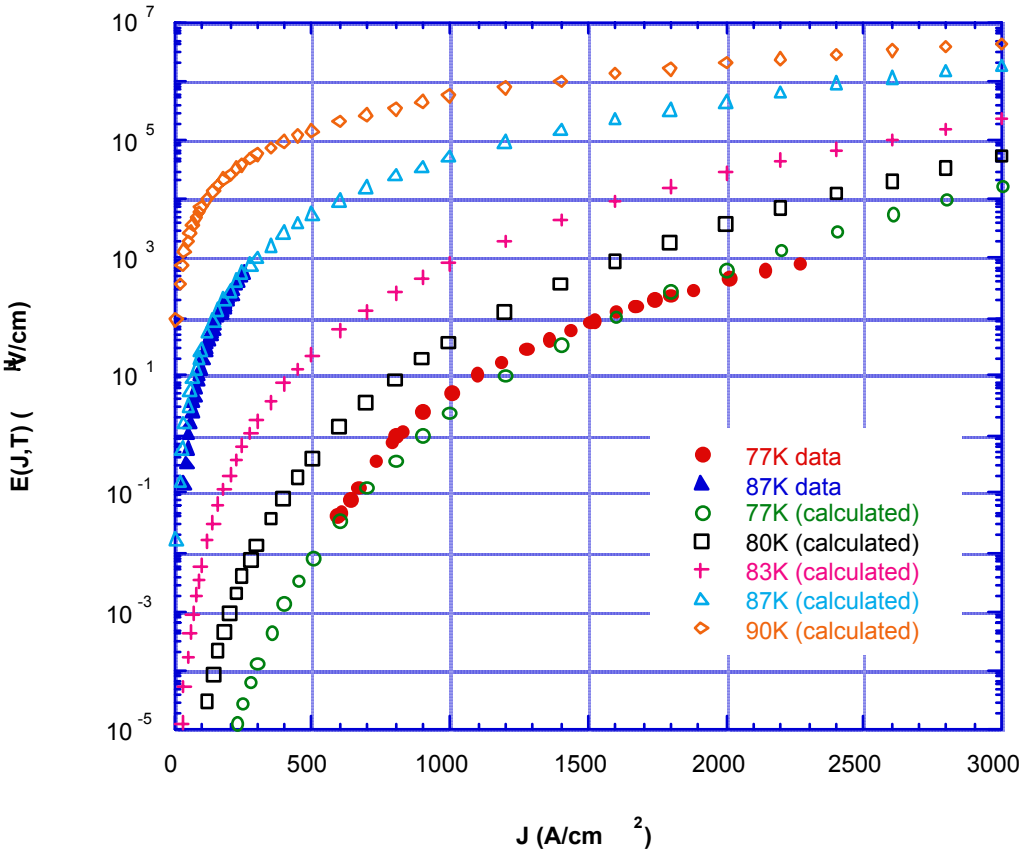

Fig. 13. Calculated E(J,T) and experimental data for melt-cast processed BSCCO-2212 rod at 77 and 87 K.

References

1. Quarterly Report for the Period Ending March 31, 2002, Practical Superconductor Development for Electrical Power Applications.

2. Quarterly Report for the Period Ending September 30, 2001, Practical Superconductor Development for Electrical Power Applications.

3. Quarterly Report for the Period Ending March 31, 2001, Practical Superconductor Development for Electrical Power Applications.

4. B. Ma, et al., Fabrication of Biaxially Textured Buffer Films on ISD MgO Templates by Pulsed Laser Deposition, submitted to *Physica C*, (2002).

5. Y. S. Cha, Magnetic Diffusion in High-T_c Superconductors, Physica C, 330 (2000) 1-8.

6. Y. S. Cha and T. R. Askew, Transient Response of a High-Temperature Superconductor Tube to Pulsed Magnetic Fields, Physica C, 302 (1998) 57-66.

7. Y. S. Cha, Magnetic Diffusion and Dissipation in High-T_c Superconductors Subjected to Sinusoidal Applied Fields, Physica C, 361 (2001) 1-12.

8. Terasaki, Y. Yanagi, Y. Itoh, M. Yoshikawa, T. Oka, H. Ikuta, U. Mizutani, Flux Motion During Pulsed-Field Magnetization in Melt-Processed YBCO, Advances in Superconductivity X, Proc. 10th Int. Symp. on Superconductivity 2, 945-948, Gifu, Japan, Oct. 27-30, 1997.

9. Y. Itol, Y. Yanagi, U. Mizutani, Flux Motion During Pulsed Field Magnetization in Y-Ba-Cu-O Superconducting Bulk Magnet, J. Appl. Phys. 82 (11) (1997) 5600-5611.

10. U. Mizutani, T. Oka, Y. Itol, Y. Yanagi, M. Yoshikawa, H. Ikuta, Pulsed-Field Magnetization Applied to High-T_c Superconductors, Appl. Supercond. 6 (2-5) (1998) 235-246.

11. Y. Yeshurun, A. P. Malozemoff, and A Shaulov, Magnetic Relaxation in High-Temperature Superconductors, Rev. Modern Phys., Vol. 68, No. 3 (1996) 911-949.

12. Y. S. Cha, S. Y. Seol, D. J. Evans, and J. R. Hull, Flux–Flow Resistivity of Three High-Temperature Superconductors, IEEE Trans. Appl. Supercond., Vol. 7, No. 2 (1997) 2122-2125.

13. Y. S. Cha, An Empirical Correlation for E(J,T) of a Melt-Cast Processed BSCCO-2212 Superconductor under Self-Field, paper presented at the 2002 Applied Superconductivity Conference, Houston, Texas, August, 2002.

Interactions

Steve Dorris, Beihai Ma, Ken Gray, Vic Maroni, John Hull, and Balu Balachandran attended the HTSC Annual Peer Review Meeting in Washington DC, July 17-19, 2002 and made presentations.

Balu Balachandran made a presentation on the current status of HTSC technology to Argonne's Strategic Partnership Committee on July 29, 2002.

Vic Maroni, Karthik Venkataraman, and Balu Balachandran attended the MRS workshop on high-temperature superconductors and made presentations at Gatlinburg, TN, Aug. 1-2, 2002.

John Hull, Y.S. Cha, Beihai Ma, and Balu Balachandran attended the Applied Superconductivity conference and made presentations in Houston, TX, Aug. 5-9, 2002.

Dr. Endo and Dr. Yamanashi, Superconductivity Research Laboratory, Advanced Institute of Science and Technology, Tsukuba, Japan visited Argonne on Aug. 13, 2002.

Prof. David Srolovitz, Princeton University visited Argonne and gave a seminar on the ion-beam-deposition process on Aug. 27, 2002.

Publications and Presentations

Published/Presented

U. Balachandran, B. Ma, M. Li, B. L. Fisher, R. E. Koritala, R. A. Erck, and S. E. Dorris, Inclined-Substrate Deposition of Biaxially Textured Template for Coated Conductors, Physica C, 378-381 , 950-954 (2002).

B. Ma, M. Li, B. L. Fisher, R. E. Koritala, and U. Balachandran, Inclined-Substrate Deposition of Biaxially Aligned Template Films for YBCO-Coated Conductors, Physica C 382, 38-42 (2002).

B. Ma, M. Li, R. E. Koritala, B. L. Fisher, S. E. Dorris, V. A. Maroni, D. J. Miller, and U. Balachandran, Direct Deposition of YBCO on Polished Ag Substrates by Pulsed Laser Deposition, Physica C, 377, 501-506 (2002).

B. Ma, M. Li, B. L. Fisher, R. E. Koritala, R. A. Erck, S. E. Dorris, and U. Balachandran, Biaxially Aligned Template Films Fabricated by Inclined-Substrate Deposition for YBCO-Coated Conductor Applications, Presented at the Applied Superconductivity Conf., Houston, TX, Aug. 4-9, 2002.

L. Chen, H. Claus, A. P. Paulikas, H. Zheng, and B. W. Veal, Joining of Melt-Textured YBCO: A Direct Contact Method, Presented at the Intl. Workshop on the Processing and Applications of Superconducting (RE)BCO Large Grain Materials, Seattle, July 11-13, 2002.

U. Balachandran, An Overview of ANL Superconductivity Program, Oral presentation to the SPC Meeting, Argonne National Laboratory, July 29, 2002.

U. Balachandran, Argonne National Laboratory Overview - ANL Superconductivity Program, Oral presentation at the DOE Annual Peer Review - Superconductivity Program for Electric Systems, Washington, DC, July 17-19, 2002.

U. Balachandran and B. Ma, Coated Conductors by Inclined Substrate Deposition Technique, Oral presentation at the DOE Annual Peer Review - Superconductivity Program for Electric Systems, Washington, DC, July 17-19, 2002.

J. Hull and A. Day (Boeing), Development of Flywheel Energy System, Oral presentation at the DOE Annual Peer Review - Superconductivity Program for Electric Systems, Washington, DC, July 17-19, 2002.

V. Maroni, A. Malozemoff (ASC), T. Holesinger (LANL), and D. Larbalestier (U. Wisc.) Wire Development Group, Oral presentation at the DOE Annual Peer Review - Superconductivity Program for Electric Systems, Washington, DC, July 17-19, 2002.

V. Maroni and K. Gray, Coated Conductor Characterization Studies, Oral presentation at the DOE Annual Peer Review - Superconductivity Program for Electric Systems, Washington, DC, July 17-19, 2002.

R. E. Koritala, D. J. Miller, B. Ma, M. Li, B. L. Fisher, and U. Balachandran, Texture Development of MgO Buffer Layers Grown by Inclined Substrate Deposition, Presented at the Applied Superconductivity Conf., Houston, TX, Aug. 4-9, 2002.

M. B. Dickerson, K. Pathak, J. Nash, K. H. Sandhage, R. L. Snyder (Ohio State U.); U. Balachandran, B. Ma; R. Blaugher, and R. Bhattacharya (NREL), Rapid HTXRD Analysis of Phase Evolution in Ceramic Materials, Presented at the Intl. Union of Crytallography Triennial Conf., Geneva, Switzerland, Aug. 4-14, 2002.

Y. S. Cha, An Empirical Correlation for E(J,T) of a Melt-Cast-Processed BSCCO-2212 Superconductor under Self Field, Presented at the Applied Superconductivity Conf., Houston, TX, Aug. 4-9, 2002.

T. R. Askew, J. M. Weber (Kalamazoo College); Y. S. Cha, H. Claus, and B. V. Veal, Transient Response of Single-Domain Y-Ba-Cu-O Rings to Pulsed Magnetic Fields, Presented at the Applied Superconductivity Conf., Houston, TX, Aug. 4-9, 2002.

S. Hanany, T. Matsumura, B. Johnson, T. Jones (U. of Minnesota); J. R. Hull; and Ki B. Ma (Texas Ctr. for Superconductivity), Use of Superconducting Bearings to Measure the Polarization of the Cosmic Microwave Background Radiation, Presented at the Applied Superconductivity Conf., Houston, TX, Aug. 4-9, 2002.

Submitted

U. Balachandran, B. Ma, M. Li, B. L. Fisher, R. E. Koritala, D. E. Miller, and S. E. Dorris, Development of Coated Conductors by Inclined Substrate Deposition, Invited abstract to be presented at the Intl. Symp. on Superconductivity (ISS 2002), Yokohama, Japan, Nov. 11-13, 2002.

M. Li, B. Ma, R. E. Koritala, B. L. Fisher, K. Venkataraman, and U. Balachandran, Pulsed Laser Deposition of YBCO Thin Films on IBAD-YSZ Substrates, Submitted to Superconductor Science and Technology (July 2002).

R. E. Koritala, D. J. Miller, B. Ma, M. Li, B. L. Fisher, and U. Balachandran, Texture Development of MgO Buffer Layers Grown by Inclined Substrate Deposition, Presented at the Applied Superconductivity Conf., ASC 2002, Aug. 4-9, 2002; to be published in IEEE Trans. Appl. Supercond.

M. B. Dickerson, K. Pathak, J. Nash, K. H. Sandhage, R. L. Snyder (Ohio State U.); U. Balachandran, B. Ma; R. Blaugher, and R. Bhattacharya (NREL), In Situ HTXRD Analysis for Rapid Determination of Processing Conditions, Abstract to be presented at the ASM Ann. Mtg., Columbus, OH, Oct. 6-10, 2002.

J. R. Hull, Flywheels, Contribution to the Encyclopedia of Energy, Elsevier Science, Academic Press, ed. C. Cleveland, 2003.

2000-2002 Patents

Metallic Substrates for High-Temperature Superconductors
T. Truchan, D. Miller, K. C. Goretta, U. Balachandran, and R. Foley (U. of IL)
U.S. Patent No. 6,455,166 (Sept. 24, 2002)

Method of Manufacturing a High Temperature Superconductor with Improved Transport Properties
Uthamalingam Balachandran, Richard Siegel, and Thomas Askew
U.S. Patent No. 6,191,075 (February 20, 2001).

Method and Apparatus for Measuring Gravitational Acceleration Utilizing a High Temperature Superconducting Bearing
John R. Hull
U.S. Patent 6,079,267 (June 27, 2000).

Method for Preparing High Temperature Superconductor
Uthamalingam Balachandran and Michael P. Chudzik
U.S. Patent No. 6,361,598 (March 26, 2002).

Thermomechanical Means to Improve Critical Current Density of BSCCO Tapes
Uthamalingam Balachandran, Roger B. Poeppel, Pradeep Haldar (IGC), and Lesizek Motowidlo (IGC)
U.S. Patent 6,240,619 (June 5, 2001).

Bearing Design for Flywheel Energy Storage using High-T_c Superconductors
John R. Hull and Thomas M. Mulcahy
U.S. Patent No. 6,153,958 (Nov. 28, 2000).

Shielded High-T_c BSCCO Tapes or Wires for High Field Applications
Uthamalingam Balachandran, Milan Lelovic, and Nicholas G. Eror
U.S. Patent No. 6,253,096 (June 26, 2001).